THE JOURNAL OF PHYSICAL CHEMISTRY A

pubs.acs.org/JPCA Article

Modeling Dynamic Conformations of Organic Molecules: Alkyne Carotenoids in Solution

Simona Streckaite,[▽] Mindaugas Macernis,[▽] Fei Li, Eliška Kuthanová Trsková, Radek Litvin, Chunhong Yang, Andrew A. Pascal, Leonas Valkunas,* Bruno Robert,* and Manuel J. Llansola-Portoles*

Cite This: J. Phys. Chem. A 2020, 124, 2792−2801 Read Online

ACCESS | Metrics & More | Article Recommendations | Supporting Information

ABSTRACT: Calculating the spectroscopic properties of complex conjugated organic molecules in their relaxed state is far from simple. An additional complexity arises for flexible molecules in solution, where the rotational energy barriers are low enough so that nonminimum conformations may become dynamically populated. These metastable conformations quickly relax during the minimization procedures preliminary to density functional theory calculations, and so accounting for their contribution to the experimentally observed properties is problematic. We describe a strategy for stabilizing these nonminimum conformations *in silico*, allowing their properties to be calculated. Diadinoxanthin and alloxanthin present atypical vibrational properties in solution, indicating the presence of several conformations. Performing energy calculations *in vacuo* and polarizable continuum model calculations in different solvents, we found three different conformations with values for the δ dihedral angle of the end ring ca. 0, 180, and 90° with respect to the plane of the conjugated chain. The latter conformation, a nonglobal minimum, is not stable during the minimization necessary for modeling its spectroscopic properties. To circumvent this classical problem, we used a Car−Parinello MD supermolecular approach, in which diadinoxanthin was solvated by water molecules so that metastable conformations were stabilized by hydrogen-bonding interactions. We progressively removed the number of solvating waters to find the minimum required for this stabilization. This strategy represents the first modeling of a carotenoid in a distorted conformation and provides an accurate interpretation of the experimental data.

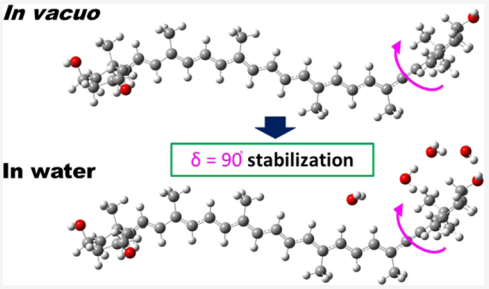

INTRODUCTION

Modeling the vibrational and electronic properties of complex conjugated organic molecules has tremendously progressed in the last 20 years because of the development of density functional theory (DFT) and time-dependent-DFT methods and their combination with quantum mechanics/molecular mechanics calculations or studies using *ab initio* molecular dynamics (QMD).[1−12] It is now possible to get quite precise estimations of the electronic and vibrational properties of such molecules and to disentangle the parameters able to tune these properties. However, for some molecules, the energy barriers to rotation around certain bonds are low enough so that nonminimum conformations become dynamically populated (in solution at room temperature, for instance). Calculating the molecular properties of these molecules using only their global energy minima may thus not fully account for the experimental observations. Similarly, it is often impossible to account for the properties of protein-bound molecules, when the binding site constrains them in a nonminimum conformation. Even though local minima can be predicted by theory, the vibrational and electronic properties of the molecules in such local minima cannot be precisely assessed—as these metastable conformations quickly relax to global minima during the energy optimization procedures defined by DFT calculations.[13−15] This constitutes a major challenge for accurately addressing the behavior of nonrigid molecules by theoretical approaches. In this paper, we report a strategy to circumvent this obstacle, which in many cases is at the origin of deviations between theoretical predictions and experimental observations.

Built from the assembly of isoprenoid units, carotenoids are one of the most important families of conjugated molecules in Nature—being present in every biological kingdom. In photosynthetic organisms, carotenoids act both as light harvesters and photoprotective molecules during the first steps of the photosynthetic process.[16,17] They represent an important player in complex biological signaling processes, as the color of a wide range of organisms is carotenoid-based.[18−22] The origin of the functional properties of carotenoids directly correlates with their linear conjugated polyene chain. A model involving three low-energy excited states has been proposed in the literature to describe their

Received: December 13, 2019
Revised: March 11, 2020
Published: March 12, 2020

https://dx.doi.org/10.1021/acs.jpca.9b11536
J. Phys. Chem. A 2020, 124, 2792−2801

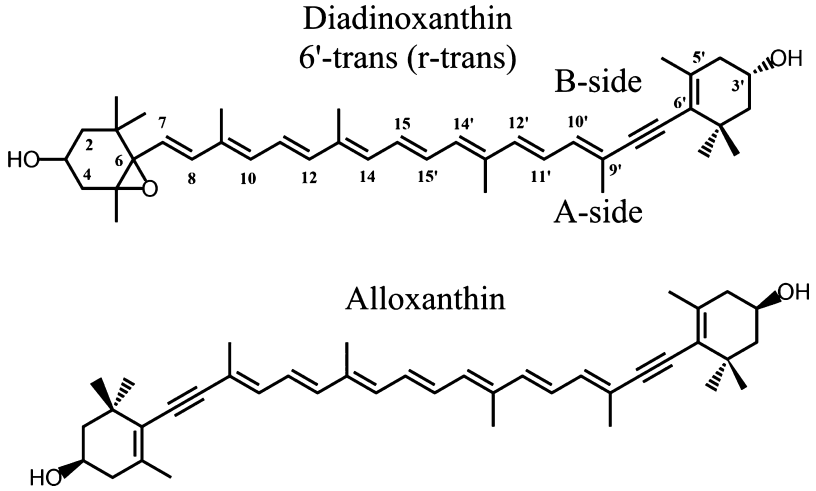

Figure 1. Molecular structures of the carotenoids studied: Ddx and Allo. The δ angle represents the dihedral angle between C10′−C9′−C6′−C5′, which characterizes the rotation of the conjugated end-ring relative to the plane of the polyene chain.

electronic properties.[23−28] Carotenoid molecules generally exhibit strong electronic absorption, arising from a transition from the ground state to the second excited state ($S_0 \rightarrow S_2$); for simplicity, we will define this transition by the energy corresponding to the lowest vibronic sublevel (0−0). The first excited state exhibits the same symmetry as the ground state and is thus optically silent (in one-photon absorption).[23] For linear carotenoids, the 0−0 transition energy tightly depends on the conjugation length.[29,30] Natural carotenoids display large structural diversity, as their carbon skeletons may include several functional groups, which may be conjugated with the isoprenoid chain (including substituted cycles). The presence of such additional conjugated groups modifies the electronic properties of these molecules and thus may tune their biological function.[16] In such cases, the vibrational and electronic properties can be related to an artificial parameter effective conjugation length (N_{eff}), defined as the number of conjugated carbon−carbon double bonds in linear carotenoids that would account for the vibrational and electronic properties of the complex carotenoid.[29,30]

Because of the isoprenoid structure, calculation of their full electronic structure and vibrational properties has proven complex even for the simplest carotenoid molecules. Considerable progress has been achieved in this field, and prediction of the electronic behavior of nondistorted carotenoids has become feasible.[31] However, carotenoids often adopt distorted conformations when bound to proteins, corresponding to out-of-plane deviations of the molecule because of rotations around C−C single bonds of the isoprenoid chain. Their precise characterization requires the analysis of their photochemistry in different solvents, which, as a basis, implicates a detailed characterization of their conformation. For β-carotene in solvent, it was recently shown that the molecule displays out-of-plane deviations of its conjugated end cycles while in some proteins, the conjugated end cycles are constrained in the molecular plane, resulting in an increase of the effective conjugation length of the molecule.[32,33] In all these cases, theoretical modeling can only address the properties of these molecules in their global minima, so that an accurate account of the influence of these distortions is not currently possible.

Diadinoxanthin (Ddx) and alloxanthin (Allo), two complex carotenoids bearing alkyne groups within the linear conjugated chain (Figure 1), are employed by some photosynthetic organisms as light-harvesting and photoprotective pigments.[34−36] In this paper, we show that the properties of these carotenoids cannot be predicted by standard DFT-based approaches because of the dynamic population of local minima. The introduction of solvent in the calculations has been shown to stabilize different minima,[37] and so we tested a new strategy based on this stabilization to model the properties of organic molecules in metastable conformations corresponding to a local minimum. In this approach, we stabilize this conformation using water molecules and perform the calculation on the carotenoid/water ensemble. The results are compared with experimental data, and the importance of such subminimal conformers is discussed.

Nomenclature. Ddx and Allo contain a conjugated cycle on one end (Ddx) or both (Allo), which may present isomerization around the carbon at position 6′ (and 6). As such isomers are distinct from isomerization in the linear chain, we distinguish them by using the nomenclature r-cis, r-trans, or r-gauche rather than the IUPAC 6′-cis, 6′-trans, or 6′-gauche[38]—where ≪r-≫ stands for ≪isomerization of the end ring relative to the linear backbone≫.

EXPERIMENTAL RESULTS

Electronic and Vibrational Properties of Ddx. The nominal conjugation length of Ddx is 10, eight C═C double bonds (alkyne) in the linear chain, and one C═C in the terminal ring after the alkyne group. Each of the alkyne carbons has two orbitals with sp hybridization and two nonhybrid p-orbitals, perpendicular to the sp orbitals and to each other. Consequently, one of these two nonhybrid p-orbitals is aligned with the nonhybrid p-orbital in the neighboring carbons either side (which show sp^2 hybridization). Thus, the conjugated chain is expected to extend through the alkyne group to the double bond in the terminal ring. C═C bonds in end rings are generally only partially conjugated, as steric hindrance causes the ring to rotate out of the plane[32,33]—although this may not be the case for Ddx, in view of the absence of the hydrogen atom on carbon C7′. Depending on the precise conformation of the end ring, we, therefore, expect a N_{eff} between 9 and 10 for this carotenoid. In order to determine the exact N_{eff}, we measured the 0−0 electronic transition of Ddx in solvents of different polar-

https://dx.doi.org/10.1021/acs.jpca.9b11536
J. Phys. Chem. A 2020, 124, 2792−2801

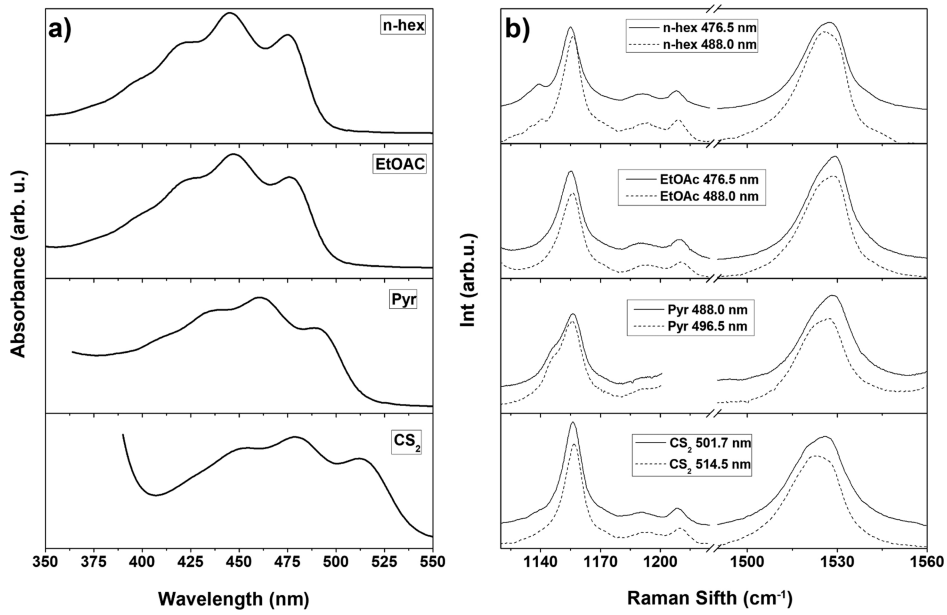

Figure 2. Room-temperature absorption (a) and resonance Raman (b) spectra of Ddx in *n*-hexane, EtOAc, pyridine, and CS_2. Two resonance Raman excitations were used, both on the red side of the 0−0 electronic transition.

izabilities (*i.e.,* *n*-hexane, ethyl acetate, pyridine, and carbon disulfide). Figure 2 shows the absorption spectra exhibiting the three characteristic vibronic bands for monomer carotenoids in solution—note that these bands appear somewhat broader than simple linear carotenoids (Supporting Information, Figure S5). The position of the 0−0 electronic transition of Ddx in each solvent is reported in Table 1—the value in *n*-hexane (21,035 cm^{-1}) is indeed between that of simple linear carotenoids spheroidene (N = 10) and neurosporene (N = 9) in *n*-hexane,[30] consistent with an N_{eff} ca. 9.5.

Table 1. Position of 0−0 Transition and ν_1 Component Maxima for Ddx in *n*-Hexane, Ethyl Acetate (EtOAc), Pyridine, and Carbon Disulphide (CS_2)

Ddx	0−0 transition	excitation (nm)	ν_{1-1} (cm^{-1})	ν_{1-2} (cm^{-1})
n-hexane	475.4 nm (21,035 cm^{-1})	476.5	1523.2	1528.9
		488.0	1524.8	1529.3
EtOAc	476.5 nm (20,986 cm^{-1})	476.5	1523.8	1529.3
		488.0	1523.5	1529.5
pyridine	489.4 nm (20,433 cm^{-1})	488.0	1522.1	1528.5
		496.5	1520.5	1527.6
CS_2	512.0 nm (19,531 cm^{-1})	501.7	1519.8	1525.9
		514.5	1519.8	1525.9

Resonance Raman, as a vibrational technique, yields direct information on the molecular properties of the carotenoid electronic ground state. The resonance Raman spectrum of carotenoids contains four main groups of bands, termed ν_1 to ν_4.[39] The main ν_1 band arises from stretching modes of the conjugated C═C bonds and gives access to the structure of the conjugated chain. Its frequency is a direct measurement of the effective conjugation length of this chain, and it has been extensively used to characterize the properties of protein-bound carotenoid molecules.[29] Simple carotenoids display a single Gaussian-like shape for this ν_1 band,[30] whereas Ddx displays a double ν_1 peak at both excitation wavelengths, and in all solvents used (Figure 2b). We observe that both components of the ν_1 band downshift together toward lower energies as the polarizability of the solvent increases, as for the single-component ν_1 of "standard" carotenoids.[30] Typically, the presence of more than one component in this spectral region is attributed to a mixed carotenoid population. However, additional purification steps, or isolation by a different protocol, still resulted in this apparently mixed population (data not shown), which thus does not result from the presence in the sample of another carotenoid species. Resonance Raman spectra recorded at two different excitation energies, both on the red side of the 0−0 transition, may be used to isolate individual carotenoids with shifted relative absorption within a mixed population, even when the mixture represents different conformers of the same carotenoid.[40] The lower frequency component of the ν_1 band clearly gains intensity when shifting the excitation toward the red, revealing that this component arises from a Ddx conformation with a slightly red-shifted absorption. The ν_2 region, which arises from stretching vibrations of C−C single bonds coupled with C−H in-plane bending modes, constitutes a fingerprint for carotenoid C−C backbone isomerization (cis/trans).[41−43] For Ddx in all solvents, this region does not show any consistent sign of isomerization, which would be marked by a satellite band ca. 1130−1140 cm^{-1} appearing in the entire set of solvents. Hence, we can conclude that there is no isomerization in the main carotenoid C−C backbone, and Ddx is in the all-trans configuration.

Resonance Raman spectra of Ddx in pyridine were measured at low temperature (77 K) using a range of excitations across the 0−0 electronic transition (Figure 3). At low temperature, the doublet character of the ν_1 band disappears, resulting in a shape similar to that observed for regular carotenoids. However, the precise position of the ν_1 is highly excitation-dependent, gradually shifting from 1532.6 to 1527.8 cm^{-1} upon shifting the excitation from 488.0 to 514.5 nm. This is

https://dx.doi.org/10.1021/acs.jpca.9b11536
J. Phys. Chem. A 2020, 124, 2792−2801

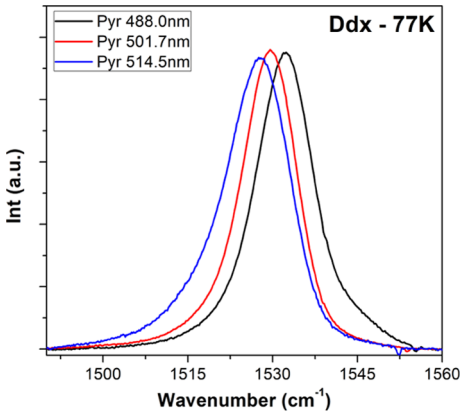

Figure 3. Resonance Raman spectra in the ν_1 region of Ddx in pyridine at 77 K for excitations at 488.0, 501.7, and 514.5 nm.

Table 2. Positions of 0−0 Transition and ν_1 Band Components for Allo in *n*-Hexane, Ethyl Acetate, Pyridine, and Carbon Disulphide at Room Temperature

Allo	0−0 transition	excitation (nm)	ν_{1-1} (cm^{-1})	ν_{1-2} (cm^{-1})
n-hexane	481.4 nm (20,773 cm^{-1})	488.0	1524.0	1530.7
		496.5	1523.4	1530.4
EtOAc	483.6 nm (20,678 cm^{-1})	488.0	1524.4	1530.8
		496.5	1523.6	1529.8
pyridine	498.9 nm (20,044 cm^{-1})	496.5	1523.1	1529.5
		501.7	1522.8	1528.4
CS_2	512.1 nm (19,527 cm^{-1})	501.7	1520.3	1528.0
		514.5	1520.2	1527.5

fully consistent with the mixture of Ddx conformations concluded from the experiments at room temperature. As the electronic transition narrows upon lowering the temperature, the resonance effect becomes more selective, and only one of the carotenoid conformers is observed in the resonance Raman spectra for each excitation. Hence, shifting the excitation results in the selective enhancement of different carotenoid species, inducing the observed shift in ν_1 band frequency.

Electronic and Vibrational Properties of Allo. We investigated Allo in order to determine whether the observed ν_1 doublet is specific for Ddx or is rather a feature of alkyne carotenoids. Allo is a carotenoid with seven C═C double bonds and two alkyne groups in the linear chain, as well as two conjugated terminal rings (Figure 1). The absorption spectra of Allo in solvents of different polarizabilities (*n*-hexane, EtOAc, pyridine, and CS_2) are shown in Figure 4a; the values of the 0−0 transition for each solvent are reported in Table 2. The nominal conjugation length of Allo is 11, but the position of the 0−0 electronic transition of Allo (20,773 cm^{-1}) is at slightly higher energy than spheroidene (20,644 cm^{-1}), indicating an effective conjugation length, a little shorter than 10. The resonance Raman spectra of this alkyne carotenoid display the same features as Ddx—a splitting of the ν_1 at room temperature, where the relative intensity of the two components is excitation-dependent. The positions of the ν_1 maxima are located at 1523 and 1530 cm^{-1} in *n*-hexane, corresponding to effective conjugation lengths close to 10 and 9, respectively. As for Ddx, the $\Delta\nu_1$ between these two peaks for Allo seems to remain constant for all solvents used, within experimental error (±0.5). The ν_2 region for Allo shows no sign of cis-isomerization in any solvent, indicating that Allo is in the all-trans configuration. As both these carotenoid molecules display the same unusual ν_1 properties, we conclude that they are associated with the presence of the alkyne group in the conjugated C═C double bond chain. The doublet must be an intrinsic feature of alkyne carotenoids in solvents, and each of the ν_1 components corresponds to a different conformation with slightly different effective conjugation length. It was recently reported that the conformation of the

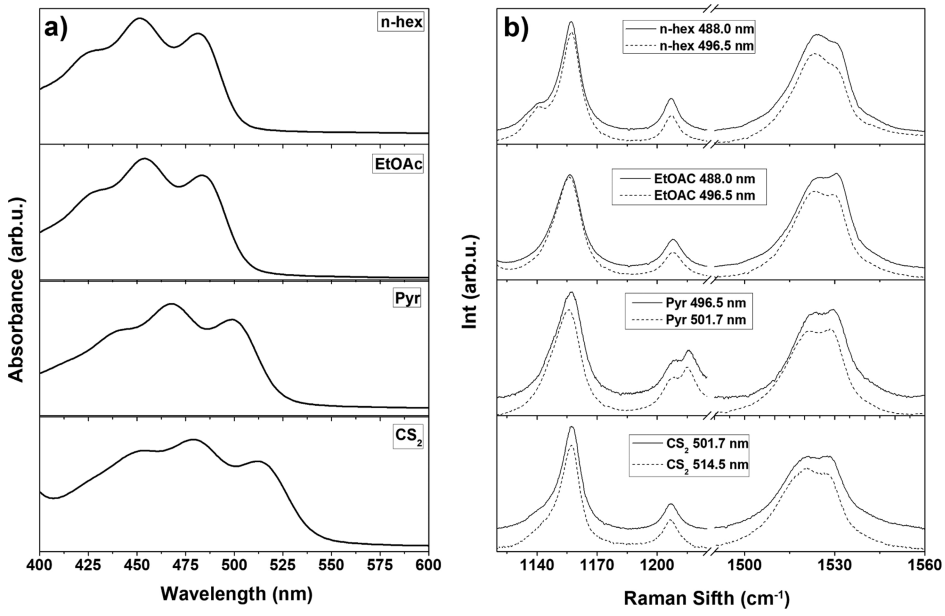

Figure 4. Room-temperature absorption (a) and resonance Raman (b) spectra of Allo in *n*-hexane, EtOAc, pyridine, and CS_2. Both Raman excitations were located on the red side of the 0−0 electronic transition.

https://dx.doi.org/10.1021/acs.jpca.9b11536
J. Phys. Chem. A 2020, 124, 2792−2801

conjugated end cycles of β-carotene had an influence on the frequency of the Raman ν_1 band of this molecule.[32,33] It is therefore reasonable to consider whether the doublet has its origin in different conformations involving the conjugated end ring(s).

THEORETICAL MODELING OF DDX

***In Vacuo* Calculations.** We performed extensive simulations of Ddx in order to comprehend the physical origin of the uncommon ν_1 doublet in alkyne carotenoids. Only all-trans conformers were modeled, as the experimental data for Ddx showed no sign of cis-isomerization for any solvent (no satellite bands ca. 1130−1140 cm^{-1} in Raman spectra; see above). We first simulated all-trans Ddx molecules *in vacuo* using the B3LYP/cc-pVDZ method.[31,44] The complex electronic structure of carotenoids, with at least three lowest exited states with perturbed symmetries $1^1A_g^-$ (forbidden), $1^1B_u^-$ (forbidden), and $1^1B_u^+$ (strongly allowed), makes the calculation of the excited states somewhat complex. The determination of the lowest excited states can be predicted by involving the highest three occupied molecular orbitals [highest occupied molecular orbital (HOMO), HOMO − 1, and HOMO − 2] and the lowest three unoccupied ones [lowest unoccupied molecular orbital (LUMO), LUMO + 1, and LUMO + 2] in the calculation, as described elsewhere.[13−15] The B3LYP approach with CAM corrections yields a theoretical energy value for the $S_0 \rightarrow S_2$ transition of 2.6 eV (476.3 nm), and a resonance Raman spectrum containing a monomodal ν_1 band similar to that usually observed for simple carotenoid molecules (1566.1 cm^{-1}). Hence, the monomodal ν_1 band obtained in the calculations establishes that the alkyne group does not induce a combination of C═C modes, leading to the experimentally observed split of the ν_1 band. The ν_1 frequency is primarily sensitive to the structure of the C═C conjugated chain, which depends in part on the precise cis/trans configuration of the molecule. The experimental resonance Raman spectrum (Figure 2) reveals that Ddx is in an all-trans configuration, so a change in configuration of the C−C backbone is excluded as the origin of the ν_1 doublet. However, it is possible that changes in the conformation of the conjugated end cycle alter the effective conjugation length of Ddx. We searched for possible conformations of the Ddx molecule that could account for this split, analyzing the minimal conformation of the alkyne end group of Ddx. As the triple bond is rigid, we studied in particular the conformation of the carbon atoms labeled C10′−C9′−C6′−C5′ (Figure 1) described by the dihedral angle (δ), which primarily represents the rotation angle around the C−C bonds either side of the triple bond. The two possible stable minima involving the end-cycle positions calculated *in vacuo* are shown in Figure 5a (see also Supporting Information, Figure S1), δ = 183.15° (r-trans type) and δ = 7.88° (r-cis type).

We took these two conformations as starting points to calculate the ground-state energy of Ddx upon rotation of the dihedral angle (δ) between C10′−C9′−C6′−C5′. We observed two stable minima for δ values close to 180° (r-trans type) and 0° (r-cis type) (Figure 5b). These two values correspond to an in-plane position of the ring on one side of the triple bond relative to the polyene chain on the other, with an energy barrier for conversion between them lower than 0.1 eV. It is worth noting that this represents only ca. 30% of the energy barrier calculated for standard carotenoids with

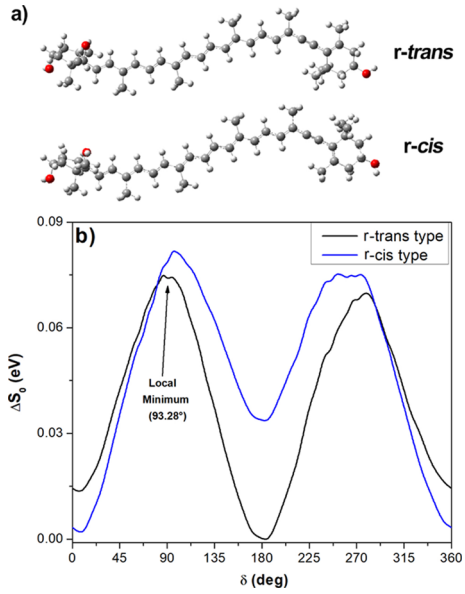

Figure 5. (a) Two minimized conformations for Ddx *in vacuo*, r-trans (δ = 183.15°), and r-cis (δ = 7.88°). (b) Relative ground-state energies according to the end group and polyene chain position, upon rotation from the minimized starting conformations in (a). δ is the dihedral angle between C10′−C9′−C6′−C5′ (see Figure 1). The arrow marks an example of the many unstable local minima found *in vacuo*.

conjugated end cycles (*e.g.* β-carotene[45]), implying that this isomerization can occur more easily for Ddx. The calculated C═C stretching frequency of Ddx in these two conformations is practically the same: 1566.1 cm^{-1} (r-trans type) and 1566.2 cm^{-1} (r-cis type). Hence, these conformations do not explain the ν_1 doublet observed experimentally. Interestingly, a number of local minima are observed, independently of the initial optimized molecular structure, in the 80−100 and 270−300° ranges of the dihedral angle (e.g., δ = 93.28°, indicated in Figure 5b). However, the vibrational and electronic properties of such r-gauche-type conformations[38] cannot be calculated because they are unstable—evolving toward the r-trans or r-cis conformation upon minimization.

Simulations in the Presence of Solvent. The untestable conformation(s) of the alkyne group observed *in vacuo* represents a potential candidate to explain the experimental properties of Ddx. To attempt to stabilize these local minima, we first performed polarizable continuum model (PCM) simulations in different solvents. These calculations in acetonitrile, *n*-hexane, and pyridine gave similar results to those obtained *in vacuo* (data not shown). They reveal the presence of several dihedral angle conformations with local minima in the 80−100 and 270−300° ranges of the dihedral angle but they were unstable and evolved toward the two global minima (r-cis or r-trans conformation). We, therefore, attempted a supermolecular approach to stabilize the structures at their local minima using hydrogen bonds from water molecules.[37] We generated a Ddx molecule in one of these r-gauche conformations (δ = 93.28°) and solvated it with 139 water molecules using the PACKMOL package.[46] We then performed Car−Parrinello molecular dynamics (QMD) on this ensemble and obtained the time-dependent evolution of the dihedral δ angle at 300 K (Figure 6). This angle presents fluctuations around 90° over the 1.5 ps timescale of the simulation, confirming that the 139 water molecules are indeed

https://dx.doi.org/10.1021/acs.jpca.9b11536
J. Phys. Chem. A 2020, 124, 2792−2801

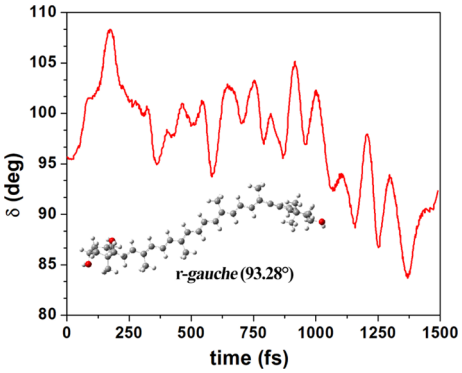

Figure 6. Collected data for static modeling: temporal evolution of the δ dihedral angle of Ddx surrounded by 139 water molecules; Car–Parrinello MD calculations at 300 K. Inset: Stable minimum with the conjugated end ring in r-gauche conformation.

able to stabilize this r-gauche conformation—δ remains within the range 80–110°, rather than evolving toward 0/180°.

To determine the minimum number of water molecules required to stabilize the r-gauche conformation, we first removed those waters not immediately surrounding the alkyne-side terminal ring, keeping 29 water molecules solvating both sides of this ring and two water molecules in the opposite nonconjugated ring. This ensemble (r-gauche Ddx + 31 HOH) was then optimized by DFT, confirming that the r-gauche conformation remained stable (Supporting Information, Figure S2). We then further reduced the number of water molecules progressively, first on side A and then on side B of the ring (see Figure 1). In each case, the ensemble structure was minimized, and the stabilized r-gauche conformation was then used to calculate the dihedral angle and the ν_1 band position (Supporting Information, Table S1). All structures with characteristic imaginary frequencies, and those which reverted to the r-cis or r-trans structures as a result of the optimization procedure, were excluded from the analysis. During the optimization procedure of the Ddx structure, the water molecules were fixed as defined from QMD calculations. This process led to a number of r-gauche structures stabilized by only a few water molecules—an example of such an ensemble, with only five solvating water molecules on side B and δ = 90.35°, is given in the Supporting Information, Figure S2.

Stabilizing the r-gauche conformation with a minimal number of water molecules then allowed us to calculate the electronic and vibrational properties of this conformer and compare them with the properties of the r-trans (183.18°) and r-cis (7.88°) conformers *in vacuo* (see above). For each structure, we determined the molecular orbitals involved in the $S_0 \rightarrow S_2$ transition: HOMO, HOMO − 1, HOMO − 2, LUMO, LUMO + 1, and LUMO + 2 (Supporting Information, Figure S3). These π-orbitals are localized principally on the polyene chain but extended to the ring C=C for the r-trans and r-cis conformers—as observed previously for carotenoids with conjugated terminal rings.[13,31] On the other hand, the r-gauche conformer exhibits remarkably different HOMO − 2 and LUMO + 2 π-orbitals, involving the end ring and only extending up to the triple bond (Figure 7). The HOMO, HOMO − 1, LUMO, and LUMO + 1 orbitals also exhibit differences from the cis and trans conformations, extending the length of the polyene chain but ending at the alkyne group (Supporting Information, Figure S2). Hence, the electronic

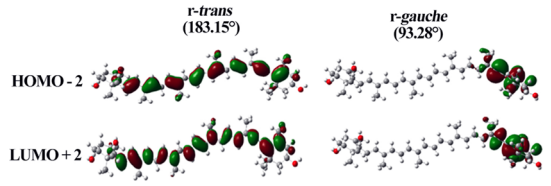

Figure 7. Molecular orbitals presenting significant changes, HOMO − 2 and LUMO + 2, for Ddx in conformations r-trans (*in vacuo*) and r-gauche (stabilized by five waters). The entire ensemble of molecular orbitals is in the Supporting Information, Figure S2.

and vibrational properties of this conformer may be significantly different because the HOMO − 2 and LUMO + 2 orbitals have significant influence on these properties. We calculated the six molecular orbitals for several of the r-gauche conformers, where the water molecules were at different positions (Supporting Information, Table S1). The Raman ν_1 frequencies calculated for each of the r-gauche structures are ca. 1570 cm^{-1}—around 6 cm^{-1} higher than that observed for the global minima *in vacuo* (r-cis or r-trans, 0/180°). The calculated pairs of values ($S_0 \rightarrow S_2$ and ν_1) for each r-gauche Ddx conformer, according to δ angle value and number of water molecules, are reported in Table 3. It is worth noting

Table 3. Calculated Position of $S_0 \rightarrow S_2$ and ν_1, According to δ Dihedral Angle, for r-Gauche Ddx Stabilized by Water Molecules

water molecules	δ (deg)	$S_0 \rightarrow S_2$ (nm)[a]	ν_1 frequency (cm^{-1})
0[b]	183.18	476.26	1566.09
4	180.74	477.13	1565.91
5	74.82	462.41	1571.24
5	78.91	460.87	1571.81
5	83.23	460.53	1571.83
5	90.35	460.52	1571.76

[a]CAM functional corrections involved in calculations. [b]*In vacuo*

that, as each of the calculated structures are surrounded by water molecules at different positions, and the $S_0 \rightarrow S_2$ state is sensitive to the presence of solvent, the calculated values are merely indicative of the tendencies in these shifts. The largest calculated difference between planar and r-gauche-type conformers of Ddx is 16 nm but this may vary depending on the nature of the solvent used for stabilization.

DISCUSSION AND CONCLUSIONS

In this paper, we have designed a strategy for calculating the spectroscopic properties of complex, conjugated molecules in nonminimum conformations and have applied this strategy to account for the properties of alkyne carotenoids in solvents. These carotenoids (Ddx and Allo) both exhibit an effective conjugation length shorter than that deduced from their structure, and resonance Raman spectra exhibit an abnormal split ν_1 band. DFT calculations, performed on Ddx minimized structures, suggest that the presence of the alkyne group does not induce any large redistribution in the C=C stretching modes that could explain the observed ν_1 splitting. The relative contributions of the two ν_1 components vary according to the excitation conditions, suggesting the presence of populations with slightly shifted absorption transitions in all solvents studied. At low temperature, the ν_1 band becomes sharper and highly excitation-dependent, again suggesting the presence of

https://dx.doi.org/10.1021/acs.jpca.9b11536
J. Phys. Chem. A 2020, 124, 2792–2801

different conformations of these molecules with slightly shifted absorption maxima. We concluded that mixtures of alkyne carotenoid conformations occur in solvents—we therefore set out to model these conformations.

The energy calculations performed *in vacuo* on Ddx suggest that this carotenoid may present conformations with values of the δ dihedral angle of the end ring close to 0/180° (flat positions) and 90/270° (perpendicular positions). The Ddx conformation corresponding to $\delta = 90°$ was not stable *in vacuo* during minimization, rendering calculation of its electronic and vibrational properties impossible. The ground-state energies of carotenoids may differ considerably in vacuum and in solvents because of the presence of heteroatoms. We therefore performed PCM calculations on Ddx solvated by water, pyridine, acetonitrile, and *n*-hexane molecules. PCM optimization of the r-gauche structure could not be achieved in any solvent—with the exception of water (see below)—because the barriers separating the relevant local r-gauche minima were very small (see Figures 5 and Supporting Information S4). Water is not an ideal solvent for hydrophobic molecules, but it exhibits a marked ability to form hydrogen bonds—which may interact with the molecule in such a way as to stabilize new conformations. Car−Parinello molecular dynamics allowed the determination of an r-gauche conformation stabilized by waters, which was then progressively desolvated. As a result, we obtained Ddx accompanied by a small number of water molecules in r-gauche conformations with slightly different values of the dihedral angle. These conformations were stable enough to allow an extensive set of DFT calculations to be performed, allowing us to model the changes in electronic and vibrational properties of Ddx, according to δ. Calculation of the orbitals of r-gauche Ddx generated HOMO − 2 and LUMO + 2 orbitals located on the end grouping involving the alkyne bond (Supporting Information, Figure S3), whereas they are expected along the conjugated chain (see other orbitals in Figure S3). Thus, where high-accuracy quantum chemistry calculations are required, such as EOM-CCSD, CASSCF or SAC-CI, these should be applied with larger orbital windows or with differentially reorganized π-orbitals for the r-gauche Ddx case. To apply the simplest semi-empirical method, we use six orbital windows to predict the perturbed symmetry states $1^1A_g^-$ and $1^1B_u^-$.[13] Some carotenoids in solvents exhibit so-called intramolecular charge transfer (ICT) states.[47] However, these do not appear in our calculations, suggesting that ICT states are not present in Ddx conformers.

The ν_1 band splitting observed experimentally is consistently larger for Allo than for Ddx molecules (see Tables 1 and 2). As follows from our model calculations, this splitting value should strongly depend on the angle between the polyene chain and the end ring (Supporting Information, Table S1), as a result of different stabilization of the structure by solvent molecules. The QMD (Figure 6) may be a good tool for searching the relevant structures in different local minima for longer times, in order to fine-tune these angles in future calculations on other systems. Experimentally, Ddx in *n*-hexane exhibits the $S_0 \rightarrow S_2$ transition at 475.4 nm and ν_1 values at 1523.2 and 1528.9 cm^{-1}. Using the CAM-B3LYP/cc-pVDZ calculation level for r-gauche (five waters) and r-cis (*in vacuo*), the values obtained were (460.5 nm, 1571.4 cm^{-1}) and (477.1 nm, 1565.9 cm^{-1}), respectively. The results show that the r-gauche conformation of the terminal ring has a direct effect on the frequency of the ν_1 C=C stretching band, upshifting it by 6 cm^{-1}. The calculations also describe the effect the r-gauche conformation has on the $S_0 \rightarrow S_2$ transition consistently, with a calculated downshift of 10−16 nm relative to r-cis. The absorption spectra recorded for Ddx and Allo in different solvents do not present any obvious features indicating the presence of different conformers. We simulated the absorption spectra of such mixtures, for several ratios of all-trans lycopene and red-shifted all-trans lycopene—the latter red-shifted by 15 nm, as estimated for a ν_1 difference of 5 cm^{-1} (Supporting Information, Figure S5).[30] These linear combinations produce absorption spectra with barely distorted features up to 8:2 mixtures, although the peaks are significantly broader—as observed experimentally for Ddx and Allo (Figure 2a). This suggests that the presence of an additional conformer at this molar ratio or less cannot be distinguished in the absorption spectrum.

On this basis, we can explain the ensemble of Ddx properties by proposing that the conjugated end ring of alkyne carotenoids in solution explores a third meta-stable conformation (in addition to the two stable, planar ones). It is of note that the QMD calculations, which led to this result, were performed in water, which is not a natural solvent for Ddx. This choice was driven purely by the notion, supported by the Car−Parinello MD, that the hydrogen bonding properties of water could stabilize a nonglobal minimum conformation sufficiently to allow this supermolecular modeling approach. To our knowledge, this is the first time that a carotenoid in a distorted conformation could be successfully modeled. It shows in particular the spectacular effect of the distortion on the molecular orbitals of the carotenoid. Predicting the properties of molecules out of their minimal conformation is a general pitfall in modeling studies, and this approach should have wide-ranging applications for QMD calculations on such distorted conformers.

MATERIALS AND METHODS

Pigment Purification. Ddx was purified from cells of the marine diatom *Phaeodactylum tricornutum* (SAG collection, strain 1090-1a). Allo was purified from cells of the marine cryptophyte *Rhodomonas salina* (strain CCAP 978/27).[48] Sample preparation was performed in the dark, on ice. Cells were separated from the culture medium by centrifugation (7000*g*, 5 min), and the pigments were extracted in three solubilization steps—in methanol twice, and finally acetone. In each step, the pellet was suspended in the solvent and sonicated to induce pigment release. The cell material was then removed by centrifugation (13,000*g*, 1 min) to be used in the following step. The cell material remained colorless after the third step. The extracts were then pooled and dried under vacuum before dissolving in methanol prior to purification. The pigments were purified using an high-performance liquid chromatography (HPLC) system consisting of Pump Controller Delta 600, a manual injection system, and a PDA 2996 detector (Waters, USA). The pigments were separated on a reverse-phase Zorbax SB-C18 column (4.6 × 150 mm, 5 μm, silica-based, nonendcapped; Agilent, USA), using a linear elution gradient at a 1 mL min^{-1} flow rate. A ternary solvent system was used as follows: 0−4 min linear gradient from 100% solvent-A to 100% solvent-B, 4−18 min linear gradient from 100% B to 20% B/80% C. (Solvent-A—80/20 methanol/0.5 M ammonium acetate (aq, pH 7.2 v/v); solvent-B—90/10 acetonitrile/water; solvent-C—100% ethyl acetate).[49] The pigments were identified based on their absorption spectra and retention times. The peaks of interest were collected, dried

https://dx.doi.org/10.1021/acs.jpca.9b11536
J. Phys. Chem. A 2020, 124, 2792−2801

out in the dark under vacuum, and stored at −80 °C. The purity of the final pigment preparation was verified by HPLC using the same protocol.[49]

UV−Vis Absorption. Absorption spectra were measured using a Varian Cary E5 Double-beam scanning spectrophotometer with a 1.0 cm path length cuvette.

Resonance Raman spectra were recorded at room temperature and 77 K, and the latter with an LN2-flow cryostat (Air Liquide, France). Laser excitations at 476.5, 488.0, 501.7, and 514.5 nm were obtained with an Ar^+ Sabre laser (Coherent). Output laser powers of 10−100 mW were attenuated to <5 mW at the sample. Scattered light was focused into a Jobin-Yvon U1000 double-grating spectrometer (1800 grooves/mm gratings) equipped with a red-sensitive, back-illuminated, LN2-cooled CCD camera. Sample stability and integrity were assessed based on the similarity between the first and last Raman spectra.

Static Calculations. The B3LYP functional in combination with the 6-311G(d,p) and cc-pVDZ basis set is known to provide reasonably good geometries.[4,31] DFT-based methods are able to perform calculations of the vibrational frequency with an overall root-mean-square error of 34−48 cm^{-1}, significantly less than that reported for the MP2 theory (61 cm^{-1}).[5] A scaling factor of 0.96 is used for frequencies calculated by the B3LYP/6-31G(d) method, in order to obtain reasonable agreement with the experimental data.[5,31,44] A polar environment can cause the shift of Raman frequencies,[31] which can be determined for specific solvents by the PCM method, with a proportional shift between experiment and calculations.[6,31,37] We chose the B3LYP/cc-pVDZ method for the present study, available in the Gaussian 09 package (Rev D.01).[50] The calculations were performed with the "nosymm" keyword, disabling attempts to identify the point group of the molecule. The end-group energy surfaces were calculated by changing the dihedral angle artificially from 0 to 360° in 0.5° steps and calculating the ground-state energy. The stabilized conformations obtained after Car−Parinello molecular dynamics were used for geometry optimization and determination of energetic levels and Raman frequencies.

Molecular Dynamics Calculations. Car−Parinello molecular dynamics (QMD) calculations were carried out using NwChem program ver 6.6,[51] with the initial molecular Ddx conformer in the gas phase optimized by DFT methods. Taking this conformer as a starting structure, we rotated the end group by 90° and obtained the initial conformations for Molecular Dynamics Simulations. Water molecules were added using PACKMOL,[46] locating the packed molecules (Ddx and 139 water molecules) in a simple 40 Å × 40 Å × 40 Å cube. Car−Parrinello molecular dynamics were carried out at 300 K with a time step of 3.0 a.u. (0.07257 fs), coupled to a Nosé−Hoovwe chains thermostat[1] at a frequency of 1200 cm^{-1}. An electronic mass parameter of 450 a.u. was implemented. Electronic exchange and correlation were modeled using the gradient-corrected functional of Perdew, Burke and Ernzerhof.[2] Core electrons were treated using the norm-conserving atomic pseudopotentials (PP) of Troullier and Martins[3] while valence electrons were represented in a planewave basis set truncated at an extended energy cut-off of 20 Ry. Following the initial equilibration period, data were accrued further (1.5 ps) for the Car−Parrinello dynamics on the parent model. The data were analyzed and visualized using the Chemcraft 1.6,[52] GaussView 5.0,[50] and VMD 1.9.2[53] programs.

■ ASSOCIATED CONTENT

Supporting Information

The Supporting Information is available free of charge at https://pubs.acs.org/doi/10.1021/acs.jpca.9b11536.

Molecular structures of r-trans and r-cis Ddx, HOMO orbital of Ddx stabilized with 31 water molecules, molecular orbitals HOMO, HOMO − 1, HOMO − 2, LUMO, LUMO + 1, and LUMO + 2, in Ddx r-trans and r-cis configurations (*in vacuo*), and r-gauche configuration stabilized by five water molecules, relative ground state energies according to end group and polyene chain position, upon rotation from the minimized starting conformations in Ddx, simulation of the absorption spectra of a mixture of carotenoids with different conjugation lengths, using lycopene in *n*-hexane as the reference, HPLC chromatograms of purified pigments prior to the spectroscopic experiments, table showing Raman ν_1 frequency correlations with the δ angle position of Ddx, structure of Ddx in configuration r-gauche (93.28°), and the XYZ structure at the b3lyp/cc-pVDZ calculation level (PDF)

■ AUTHOR INFORMATION

Corresponding Authors

Leonas Valkunas − *Institute of Chemical Physics, Faculty of Physics, Vilnius University, LT-10222 Vilnius, Lithuania; Molecular Compounds Physics Department, Center for Physical Sciences and Technology, LT-10257 Vilnius, Lithuania;* orcid.org/0000-0002-1356-8477; Email: leonas.valkunas@ff.vu.lt

Bruno Robert − *Université Paris-Saclay, CEA, CNRS, Institute for Integrative Biology of the Cell (I2BC), 91198 Gif-sur-Yvette, France*; Email: Bruno.ROBERT@cea.fr

Manuel J. Llansola-Portoles − *Université Paris-Saclay, CEA, CNRS, Institute for Integrative Biology of the Cell (I2BC), 91198 Gif-sur-Yvette, France;* orcid.org/0000-0002-8065-9459; Email: manuel.llansola@i2bc.paris-saclay.fr

Authors

Simona Streckaite − *Université Paris-Saclay, CEA, CNRS, Institute for Integrative Biology of the Cell (I2BC), 91198 Gif-sur-Yvette, France;* orcid.org/0000-0003-0541-5806

Mindaugas Macernis − *Institute of Chemical Physics, Faculty of Physics, Vilnius University, LT-10222 Vilnius, Lithuania*

Fei Li − *Université Paris-Saclay, CEA, CNRS, Institute for Integrative Biology of the Cell (I2BC), 91198 Gif-sur-Yvette, France; Key Laboratory of Photobiology, Institute of Botany, Chinese Academy of Sciences, 100093 Beijing, People's Republic of China*

Eliška Kuthanová Trsková − *Faculty of Science, University of South Bohemia, 370 05 Ceske Budejovice, Czech Republic; Institute of Microbiology, Academy of Sciences of the Czech Republic, 379 81 Třeboň, Czech Republic*

Radek Litvin − *Biology Centre, Czech Academy of Sciences, 370 05 Ceske Budejovice, Czech Republic; Faculty of Science, University of South Bohemia, 370 05 Ceske Budejovice, Czech Republic*

Chunhong Yang − *Key Laboratory of Photobiology, Institute of Botany, Chinese Academy of Sciences, 100093 Beijing, People's Republic of China*

https://dx.doi.org/10.1021/acs.jpca.9b11536
J. Phys. Chem. A 2020, 124, 2792−2801

Andrew A. Pascal − *Université Paris-Saclay, CEA, CNRS, Institute for Integrative Biology of the Cell (I2BC), 91198 Gif-sur-Yvette, France*

Complete contact information is available at: https://pubs.acs.org/10.1021/acs.jpca.9b11536

Author Contributions

[∇]S.S. and M.M. are equivalent authors.

Notes

The authors declare no competing financial interest.

■ ACKNOWLEDGMENTS

Spectroscopic measurements were performed on the Biophysics Platform of I2BC; computations on resources at the High-Performance Computing Center "HPC Sauletekis" in Vilnius University Faculty of Physics. The skilled technical assistance of Frantisek Matousek in purification of carotenoids is gratefully acknowledged. This work was supported by the ERC funding agency (PHOTPROT project), the French Infrastructure for Integrated Structural Biology (FRISBI) ANR-10-INBS-05, the European Union's Horizon 2020 research and innovation program under the Marie Skłodowska-Curie grant agreement no 675006 (SE2B), and Gilibert project S-LZ-19-3. The work in the Czech Republic was supported by the Czech Science Foundation projects 19-11494S (E. Kuthanová Trsková) and 31-19-28323X (R. Litvin). Institutional support RVO:60077344 and Institutional project Algatech Plus (MSMT LO1416) of the Czech Ministry of Education, Youth and Sport are also acknowledged.

■ REFERENCES

(1) Martyna, G. J.; Klein, M. L.; Tuckerman, M. Nosé−Hoover chains: The canonical ensemble via continuous dynamics. *J. Chem. Phys.* **1992**, *97*, 2635−2643.
(2) Perdew, J. P.; Burke, K.; Ernzerhof, M. Generalized Gradient Approximation Made Simple. *Phys. Rev. Lett.* **1996**, *77*, 3865−3868.
(3) Troullier, N.; Martins, J. L. Efficient pseudopotentials for plane-wave calculations. *Phys. Rev. B: Condens. Matter Mater. Phys.* **1991**, *43*, 1993−2006.
(4) Dreuw, A.; Harbach, P. H. P.; Mewes, J. M.; Wormit, M. Quantum chemical excited state calculations on pigment−protein complexes require thorough geometry re-optimization of experimental crystal structures. *Theor. Chem. Acc.* **2010**, *125*, 419−426.
(5) Wong, M. W. Vibrational frequency prediction using density functional theory. *Chem. Phys. Lett.* **1996**, *256*, 391−399.
(6) Liu, W.; Wang, Z.; Zheng, Z.; Jiang, L.; Yang, Y.; Zhao, L.; Su, W. Density Functional Theoretical Analysis of the Molecular Structural Effects on Raman Spectra of β-Carotene and Lycopene. *Chin. J. Chem.* **2012**, *30*, 2573−2580.
(7) Mardirossian, N.; Head-Gordon, M. Thirty years of density functional theory in computational chemistry: an overview and extensive assessment of 200 density functionals. *Mol. Phys.* **2017**, *115*, 2315−2372.
(8) Cohen, A. J.; Mori-Sánchez, P.; Yang, W. Challenges for Density Functional Theory. *Chem. Rev.* **2012**, *112*, 289−320.
(9) Chung, L. W.; Sameera, W. M. C.; Ramozzi, R.; Page, A. J.; Hatanaka, M.; Petrova, G. P.; Harris, T. V.; Li, X.; Ke, Z.; Liu, F.; Li, H.-B.; Ding, L.; Morokuma, K. The ONIOM Method and Its Applications. *Chem. Rev.* **2015**, *115*, 5678−5796.
(10) Hutter, J. Car−Parrinello molecular dynamics. *Wiley Interdiscip. Rev.: Comput. Mol. Sci.* **2012**, *2*, 604−612.
(11) Kühne, T. D. Second generation Car−Parrinello molecular dynamics. *Wiley Interdiscip. Rev.: Comput. Mol. Sci.* **2014**, *4*, 391−406.
(12) Rudberg, E.; Sałek, P.; Helgaker, T.; Ågren, H. Calculations of two-photon charge-transfer excitations using Coulomb-attenuated density-functional theory. *J. Chem. Phys.* **2005**, *123*, 184108.
(13) Macernis, M.; Sulskus, J.; Duffy, C. D. P.; Ruban, A. V.; Valkunas, L. Electronic Spectra of Structurally Deformed Lutein. *J. Phys. Chem. A* **2012**, *116*, 9843−9853.
(14) Cunningham, F. X., Jr.; Gantt, E. One ring or two? Determination of ring number in carotenoids by lycopene epsilon-cyclases. *Proc. Natl. Acad. Sci. U.S.A.* **2001**, *98*, 2905−2910.
(15) Tschirner, N.; Schenderlein, M.; Brose, K.; Schlodder, E.; Mroginski, M. A.; Hildebrandt, P.; Thomsen, C. Raman excitation profiles of β-carotene − novel insights into the nature of the ν1-band. *Phys. Status Solidi B* **2008**, *245*, 2225−2228.
(16) Britton, G.; Liaaen-Jensen, S.; Pfander, H. *Carotenoids: Natural Functions*; Birkhäuser Verlag: Switzerland, 2008; Vol. *4*.
(17) Frank, H. A.; Young, A. J.; Britton, G.; Cogdell, R. J. *The Photochemistry of Carotenoids*; Kluwer Academic Publishing, 1999.
(18) Thomas, D. B.; McGraw, K. J.; Butler, M. W.; Carrano, M. T.; Madden, O.; James, H. F. Ancient origins and multiple appearances of carotenoid-pigmented feathers in birds. *Proc. R. Soc. B* **2014**, *281*, 20140806.
(19) Zhao, C.; Nabity, P. D. Phylloxerids share ancestral carotenoid biosynthesis genes of fungal origin with aphids and adelgids. *PLoS One* **2017**, *12*, No. e0185484.
(20) Harrison, E. H.; Quadro, L. Apocarotenoids: Emerging Roles in Mammals. *Annu. Rev. Nutr.* **2018**, *38*, 153−172.
(21) Saint, S.; Renzi-Hammond, L.; Khan, N.; Hillman, J. The Macular Carotenoids are Associated with Cognitive Function in Preadolescent Children. *Nutrients* **2018**, *10*, 193.
(22) Hou, X.; Rivers, J.; León, P.; McQuinn, R. P.; Pogson, B. J. Synthesis and Function of Apocarotenoid Signals in Plants. *Trends Plant Sci.* **2016**, *21*, 792−803.
(23) Tavan, P.; Schulten, K. Electronic excitations in finite and infinite polyenes. *Phys. Rev. B: Condens. Matter Mater. Phys.* **1987**, *36*, 4337−4358.
(24) Polívka, T.; Sundström, V. Ultrafast Dynamics of Carotenoid Excited States−From Solution to Natural and Artificial Systems. *Chem. Rev.* **2004**, *104*, 2021−2072.
(25) Schulten, K.; Karplus, M. On the origin of a low-lying forbidden transition in polyenes and related molecules. *Chem. Phys. Lett.* **1972**, *14*, 305−309.
(26) Frank, H. A. Spectroscopic Studies of the Low-Lying Singlet Excited Electronic States and Photochemical Properties of Carotenoids. *Arch. Biochem. Biophys.* **2001**, *385*, 53−60.
(27) Rondonuwu, F. S.; Yokoyama, K.; Fujii, R.; Koyama, Y.; Cogdell, R. J.; Watanabe, Y. The role of the 11Bu− state in carotenoid-to-bacteriochlorophyll singlet-energy transfer in the LH2 antenna complexes from Rhodobacter sphaeroides G1C, Rhodobacter sphaeroides 2.4.1, Rhodospirillum molischianum and Rhodopseudomonas acidophila. *Chem. Phys. Lett.* **2004**, *390*, 314−322.
(28) Nishimura, K.; Rondonuwu, F. S.; Fujii, R.; Akahane, J.; Koyama, Y.; Kobayashi, T. Sequential singlet internal conversion of 1Bu+→3Ag−→1Bu−→2Ag−→(1Ag− ground) in all-trans-spirilloxanthin revealed by two-dimensional sub-5-fs spectroscopy. *Chem. Phys. Lett.* **2004**, *392*, 68−73.
(29) Llansola-Portoles, M. J.; Pascal, A. A.; Robert, B. Electronic and vibrational properties of carotenoids: from in vitro to in vivo. *J. R. Soc., Interface* **2017**, *14*, 20170504.
(30) Mendes-Pinto, M. M.; Sansiaume, E.; Hashimoto, H.; Pascal, A. A.; Gall, A.; Robert, B. Electronic Absorption and Ground State Structure of Carotenoid Molecules. *J. Phys. Chem. B* **2013**, *117*, 11015−11021.
(31) Macernis, M.; Sulskus, J.; Malickaja, S.; Robert, B.; Valkunas, L. Resonance Raman Spectra and Electronic Transitions in Carotenoids: A Density Functional Theory Study. *J. Phys. Chem. A* **2014**, *118*, 1817−1825.
(32) Mendes-Pinto, M. M.; Galzerano, D.; Telfer, A.; Pascal, A. A.; Robert, B.; Ilioaia, C. Mechanisms Underlying Carotenoid Absorption

in Oxygenic Photosynthetic Proteins. *J. Biol. Chem.* **2013**, *288*, 18758−18765.
(33) Llansola-Portoles, M. J.; Sobotka, R.; Kish, E.; Shukla, M. K.; Pascal, A. A.; Polívka, T.; Robert, B. Twisting a β-Carotene, an Adaptive Trick from Nature for Dissipating Energy during Photoprotection. *J. Biol. Chem.* **2017**, *292*, 1396−1403.
(34) Kaňa, R.; Kotabová, E.; Sobotka, R.; Prášil, O. Non-Photochemical Quenching in Cryptophyte Alga Rhodomonas salina Is Located in Chlorophyll a/c Antennae. *PLoS One* **2012**, *7*, No. e29700.
(35) Streckaite, S.; Gardian, Z.; Li, F.; Pascal, A. A.; Litvin, R.; Robert, B.; Llansola-Portoles, M. J. Pigment configuration in the light-harvesting Protein of the Xanthophyte alga Xanthonema debile. *Photosynth. Res.* **2018**, *138*, 139−148.
(36) Goss, R.; Jakob, T. Regulation and function of xanthophyll cycle-dependent photoprotection in algae. *Photosynth. Res.* **2010**, *106*, 103−122.
(37) Macernis, M.; Kietis, B. P.; Sulskus, J.; Lin, S. H.; Hayashi, M.; Valkunas, L. Triggering the proton transfer by H-bond network. *Chem. Phys. Lett.* **2008**, *466*, 223−226.
(38) Moss, G. P. Basic terminology of stereochemistry (IUPAC Recommendations 1996). *Pure Appl. Chem.* **1996**, *68*, 2193.
(39) Gill, D.; Kilponen, R. G.; Rimai, L. Resonance Raman Scattering of Laser Radiation by Vibrational Modes of Carotenoid Pigment Molecules in Intact Plant Tissues. *Nature* **1970**, *227*, 743−744.
(40) Ruban, A. V.; Pascal, A. A.; Robert, B. Xanthophylls of the major photosynthetic light-harvesting complex of plants: identification, conformation and dynamics. *FEBS Lett.* **2000**, *477*, 181−185.
(41) Koyama, Y.; Takatsuka, I.; Nakata, M.; Tasumi, M. Raman and infrared spectra of the all-trans, 7-cis, 9-cis, 13-cis and 15-cis isomers of β-carotene: Key bands distinguishing stretched or terminal-bent configurations form central-bent configurations. *J. Raman Spectrosc.* **1988**, *19*, 37−49.
(42) Koyama, Y.; Takii, T.; Saiki, K.; Tsukida, K. Configuration of the carotenoid in the reaction centers of photosynthetic bacteria. 2. Comparison of the resonance Raman lines of the reaction centers with those of the 14 different cis-trans isomers of β-carotene. *Photobiochem. Photobiophys.* **1983**, *5*, 139−150.
(43) Koyama, Y.; Kito, M.; Takii, T.; Saiki, K.; Tsukida, K.; Yamashita, J. Configuration of the carotenoid in the reaction centers of photosynthetic bacteria. Comparison of the resonance Raman spectrum of the reaction center of Rhodopseudomonas sphaeroides G1C with those of cis-trans isomers of β-carotene. *Biochim. Biophys. Acta, Bioenerg.* **1982**, *680*, 109−118.
(44) Macernis, M.; Galzerano, D.; Sulskus, J.; Kish, E.; Kim, Y.-H.; Koo, S.; Valkunas, L.; Robert, B. Resonance Raman Spectra of Carotenoid Molecules: Influence of Methyl Substitutions. *J. Phys. Chem. A* **2015**, *119*, 56−66.
(45) Liu, W.-L.; Wang, Z.-G.; Zheng, Z.-R.; Li, A.-H.; Su, W.-H. Effect of β-Ring Rotation on the Structures and Vibrational Spectra of β-Carotene: Density Functional Theory Analysis. *J. Phys. Chem. A* **2008**, *112*, 10580−10585.
(46) Martínez, L.; Andrade, R.; Birgin, E. G.; Martínez, J. M. PACKMOL: A package for building initial configurations for molecular dynamics simulations. *J. Comput. Chem.* **2009**, *30*, 2157−2164.
(47) Redeckas, K.; Voiciuk, V.; Vengris, M. Investigation of the S1/ICT equilibrium in fucoxanthin by ultrafast pump-dump-probe and femtosecond stimulated Raman scattering spectroscopy. *Photosynth. Res.* **2016**, *128*, 169−181.
(48) West, R.; Keşan, G.; Trsková, E.; Sobotka, R.; Kaňa, R.; Fuciman, M.; Polívka, T. Spectroscopic properties of the triple bond carotenoid alloxanthin. *Chem. Phys. Lett.* **2016**, *653*, 167−172.
(49) Llansola-Portoles, M. J.; Uragami, C.; Pascal, A. A.; Bina, D.; Litvin, R.; Robert, B. Pigment structure in the FCP-like light-harvesting complex from Chromera velia. *Biochim. Biophys. Acta, Bioenerg.* **2016**, *1857*, 1759−1765.
(50) Frisch, M. J.; Trucks, G. W.; Schlegel, H. B.; Scuseria, G. E.; Robb, M. A.; Cheeseman, J. R.; Scalmani, G.; Barone, V.; Mennucci, B.; Petersson, G. A. *Gaussian 09*; Gaussian, Inc.: Wallingford, CT, USA, 2009.
(51) Valiev, M.; Bylaska, E. J.; Govind, N.; Kowalski, K.; Straatsma, T. P.; Van Dam, H. J. J.; Wang, D.; Nieplocha, J.; Apra, E.; Windus, T. L.; de Jong, W. A. NWChem: A comprehensive and scalable open-source solution for large scale molecular simulations. *Comput. Phys. Commun.* **2010**, *181*, 1477−1489.
(52) Chemcraft Graphical software for visualization of quantum chemistry computations. https://www.chemcraftprog.com.
(53) Humphrey, W.; Dalke, A.; Schulten, K. VMD: Visual molecular dynamics. *J. Mol. Graphics* **1996**, *14*, 33−38.

https://dx.doi.org/10.1021/acs.jpca.9b11536
J. Phys. Chem. A 2020, 124, 2792−2801